Supporting information

Aqueous Dispersion of SWCNT using Vegetable Oil-based 3-arm Star Oligomer: Mechanistic Investigation and its Functional Application

Usashi Pal,[#a] Aashika R Nath,[#a] Devilakshmi P,[#a] Soumadip Banerjee,[b] Abhijit Kumar Das,[c] Avik Ghosh, [c]* Jit Sarkar[a,d]*

[a] Polymer Science & Technology Unit, Advanced Materials Laboratory, CSIR-Central Leather Research Institute (CSIR-CLRI) Sardar Patel Road, Adyar, Chennai 600 020, India.

[b] Graduate School of System Informatics, Kobe University, 1-1, Rokkodai-cho, Nada-ku, Kobe, 657-8501, JAPAN

[c] School of Mathematical & Computational Sciences, Indian Association for the cultivation of science, Kolkata 700032, India

[d] Academy of Scientific and Innovative Research (AcSIR), Ghaziabad 201002, India

1. Materials. Castor oil (CO, SRL, pure), glycidyl methacrylate (GMA) (Sigma-Aldrich, USA, ≥97.0%), triethylamine (TEA, Sigma-Aldrich, USA, ≥99), acetone (SDFCL, India), hexane (SDFCL, India), chloroform ($CHCl_3$, SRL, 99.5%), chloroform-*d* ($CDCl_3$, 99.8 atom% D) (Sigma-Aldrich, USA), N-Methyl-2-pyrrolidone (NMP, Fisher Scientific, 99.13), and SWCNT (TCI, .55%, >2 nm (diam.), 5-15 μm (length)) were used as purchased. Milli-Q (MQ) water was collected from Direct-Q®3 and was used for this study. Aqualen-IW-80.A (Stahl, India) (a finishing auxiliary) was collected from CSIR-CLRI tannery and utilized for the experiments.

2. Methods.

Synthesis of CG2 oligomer. CO (20 g, 1 eqv.) and TEA (10 g, 4.6 eqv.) were taken in a two-neck round bottom (RB) flask and stirred by a mechanical stirrer at r.t. for 15 min. GMA (70 g, 23 eqv.) was added to the RB flask and heated at 55 ºC for 8 h. The progress of the reaction was monitored by the change in colour of the solution from pale yellow to dark yellow to

brown. After 7 h, the reaction mixture was kept at room temperature overnight. After that, the reaction mixture was diluted with $CHCl_3$ (30 mL), precipitated from hexane (non-solvent), and this process was repeated three times. The precipitate was collected, dried at room temperature, and stored in a refrigerator for further experiments and analysis.

Preparation of SWCNTs/Polymer Dispersion. An aqueous solution of $CG2_{0.1}$ (0.1 wt%) was prepared by dissolving 20 mg of CG2 in 20 mL of MQ water. The solution was allowed to stand for 48 hours to enable complete polymer swelling and was subsequently used as the stock solution.

For the preparation of SWCNT dispersions, 1 mg of single-walled carbon nanotubes (SWCNTs) was first dispersed in 10 mL of N-methyl-2-pyrrolidone (NMP) by sonicating for 3-4 h. From this dispersion, 10 μL was added to 5 mL of MQ water to obtain a final SWCNT concentration of 0.00002 wt%. The resulting mixture was sonicated for 30 min to ensure proper dispersion. Higher concentrations of SWCNT solutions (0.0002 and 0.001 wt%) were prepared in a similar manner by appropriate dilution of the NMP dispersion.

A secondary stock solution of CG2 (0.002 wt%) was prepared from the primary stock solution. The calculated amount of CG2 solution was added from primary and secondary stock solution, to SWCNT dispersion (5 mL) and sonicated for 10 minutes to prepare the final samples for analysis. Thus, different samples were prepared and analyzed with DLS, FESEM, UV-Vis, and FTIR.

FTIR-ATR Analysis of CG2-SWCNT aqueous solutions. For FTIR-ATR measurements, a drop of the aqueous suspension containing pure $CG2_{0.004,}$ $SWCNT_{0.00002,}$ with varying CG2 concentrations (0.004–0.02 wt%), and pure MQ water was placed in the pellet holder

positioned on the diamond crystal of the ATR accessory. The spectrum of water was subtracted to eliminate interference from water absorption bands in the sample spectra.

Computational Analysis. All electronic structure and frequency calculations were performed using the Gaussian 16[1] suite of quantum chemistry program. Geometries of all the species involved were optimized by employing Density Functional Theory (DFT), considering CAM-B3LYP functional[2] in conjunction with all-electron 6-31G* basis set.

The binding energy (Δ_{BE}) was calculated using the following formula:

$$\Delta_{BE} = E[CG^*\text{-}CNT] - E[CG^*] - E[CNT] \quad (1)$$

The topology of the interaction between the metal ion and the binding sites of the oligomer were studied using the topological analysis of 'atoms in molecule' (AIM) formalism employing AIMAll program[3-5] where the classical definition of a 'bond' was modified in the form of 'bond path' which basically indicates a line of maximum electron density linking bonded pairs of atoms in an equilibrium geometry. According to Bader, every classical structure is mirrored by a molecular graph consisting of bond paths, linking neighbouring atoms. The interaction of two atoms at a certain distance creates a critical point in the electron density, where the gradient,$\nabla\rho(r)$vanishes, which is termed as bond critical point (BCP). In order to evaluate the strength of the interaction, two important parameters, viz., electron density $\rho(r)$ and its Laplacian ($\nabla^2\rho$) at the bond critical point (BCP), were calculated. For covalent bonds, the electron density at the BCP is of the order of 0.1 a.u. For non-covalent interactions, e.g., weak H-bonds and van der Waals interactions, it is lower by about 0.01 a.u. or even less. Electronic energy density [H(r)] is defined as the summation of kinetic energy, G(r) (always positive), and potential energy density, ∇ (r) (always negative), the ratio of which, i.e., - G(r)/V(r) predicts the nature of the bond. The interaction is said to be very weak or non-covalent if - G(r)/V(r) > 1 and partly covalent if 0.5 < - G(r)/V(r) < 1. Negative values of both $\nabla^2\rho$ and H(r)

indicate the interaction to be strong, for medium interaction H(r) is negative but $\nabla^2\rho$ is positive, and the interactions are weak when both are positive.

The inference drawn by AIM was further supported by the colour-filled iso-surface graphs through NCI (Non-Covalent Interaction) analysis[6] i.e., done by Multiwfn[7] and plotted by VMD[8] visualization tool. From the colour-filled RDG iso-surface, different types of interactions can be assessed by examining their colours. The bluer colour implies the stronger attractive interaction; the green/light brown indicates van der Waals or other non-covalent or weak interaction. The regions correspond to strong steric interaction have been marked by red.

Conductivity. A 0.5 mL solution of SWCNT (0.1 wt%) and CG2 (1 wt%) at a weight ratio of 1:10 (SWCNT/CG2) were prepared. Separately, a 0.5 ml solution of SWCNT (0.1 wt%) also prepared. These stock solutions were sonicated for 30 min. For conductance measurements in the solution state, 0.15 mL of each stock solution was added separately to 15 mL of water in a glass vial fitted to the conductivity meter. In each experiment, the baseline conductance of water was recorded prior to the addition of the solution, followed by measurement of the conductance after introducing 0.15 mL of $SWCNT_{0.1}$ or $CG2_1$–$SWCNT_{0.1}$.

For conductive coating, Whatman filter papers (1.5 × 1 cm) were coated with 0.5 mL of the dispersed stock solutions and conductivity were measured. The conductivity of the coated material was calculated using the formulae:[9]

$$\rho = \frac{R \times T \times W}{L} \quad \ldots\ldots\ldots\ldots\ldots\ldots\ldots\ldots (1)$$

$$\kappa = \frac{1}{\rho} \quad \ldots\ldots\ldots\ldots\ldots\ldots\ldots\ldots\ldots\ldots (2)$$

where, R is resistance, W is the width, L is the length between two electrodes, T is the thickness, ρ is the resistivity, and κ is the conductivity of the FP.

Touch-screen application. For fabricating protype gloves and demonstrating touchscreen application 25 μL of Aqualen-IW-80 (1 wt%) in $CHCl_3$ was drop-casted on $CG2_1$–$SWCNT_{0.1}$ coated FP to more stabilize the surface coating. The coated and uncoated FP was attached on the fingertip of a glove to prepare the protype glove and used for touchscreen applications.

3. Measurements

The Perkin Elmer FTIR and FTIR-ATR instruments were used to analyze functional groups using 16-32 scans at a wavenumber ranging from 4000 to 400 cm^{-1}. Eight tons of pressure were used to manufacture the sample pellets. Using a 400 MHz Avance III HD Bruker FT-NMR spectrometer, the ^1H chemical shifts of the polymer, CG2, were measured. As a solvent, CDCl3 was employed.

Dynamic light scattering (DLS) experiments were performed in the Malvern Zetasizer instrument.

GPC was analyzed using PSt-calibrated Agilent gel permeation chromatography (GPC) system where THF was eluent (flow rate = 1.0 mL/min).

The weight-average molecular weight (M_w) and $Đ$ of the CG2 were determined in a size exclusion chromatography comprising with Shimadzu LC-20AD, Shimadzu DGU-20A3R, Shimadzu CTO-20A, two numbers of PL gel 5 μm MIXED-C columns, and one guard column. The columns were calibrated by narrow polystyrene standards, and THF was used as an eluent with a flow rate of 0.8 mL/min.

Through the use of the CLARA GMU field emission scanning electron microscope (FESEM), the dispersity of SWCNT (0.00002, 0.0002, and 0.001 wt%) with $CG2_{0.004}$ polymer was observed in the solution state. FESEM images were also taken for the uncoated FP, FP-coated

$SWCNT_{0.1}$, and FP-coated $CG2_1$- $SWCNT_{0.1}$ to show the de-bundling of these nanotubes on interacting with CG2.

HRTEM images were obtained on a JEM-F200 transmission electron microscope (JEOL) operated at 200 kV. The TEM grid was a carbon film-supported copper grid (200 mesh) (Sigma Aldrich, USA). NP solution was dropped on a TEM grid and dried at room temperature. TEM analyses were done to determine the sizes of the CG2 polymer nanoparticles in the solution state and to show the dispersity of the CNTs when the polymer gets adsorbed on their walls.

UV-Vis spectroscopy was performed using the JASCO V-750 Spectrophotometer.

The resistance of these materials was measured with a DT830D Digital multimeter and conductance in the solution state was measured with the Eutech conductivity meter instrument.

4. Supplementary Tables.

Table S1. Synthesis of CO-based 3-arm star polymer (CG2).

Polymer	[CO]/[GMA]/[TEA] (eqv.)	T (ºC)	*t* (h)	M_w[a] (g/mol)	*Đ*[a]	GMA units from NMR[b]
CG2	1/23/4.6	55	8	1756	2.45	18

[a] M_w and *Đ* were obtained from the GPC. [b] No. of GMA units were calculated by comparing the peak area of terminal protons (protons h) of CO and alkene protons of GMA (protons m and n).

Table S2. Binding Energy (Δ_{BE}) and Charges of the concerned atoms, optimized at the CAM-B3LYP/6-31G* level

Geometry	Δ_{BE} (kcal/mol)	Charge (Mulliken)	
		Atom	Charge
A-1	-4.33	O_1,C_1,O_2	-0.48,0.61,-0.64
		C_a,C_b,C_c	-0.04,-0.03,-0.05
A-2	-4.93	O_1,C_1,O_3	-0.46,0.71,-0.65
		C_d,C_e,C_f	-0.08,-0.03,-0.08
A-3	-5.84	O_3	-0.65
		C_g	0.05
A-4	-5.55	C_2,C_3	-0.10,-0.08
		C_h,C_i	-0.15,-0.16
A-5	-8.21	O_1	-0.49
		C_j,C_k	-0.20,-0.20

Table S3. AIM Analysis of the geometries, optimized at the CAM-B3LYP/6-31G* Level.

System	BCP	ρ(r)	$\nabla^2\rho$	V	G	H	-(G/V)
A-1	O_1-C_a	0.0078	0.0243	-0.0046	0.0053	0.0007	1.1510
	C_1-C_b	0.0039	0.0106	-0.0016	0.0021	0.0005	1.3517
	O_2-C_c	0.0078	0.0243	-0.0040	0.0054	0.0014	1.3559
A-2	O_1-C_d	0.0078	0.0243	-0.0047	0.0054	0.0007	1.1478
	C_1-C_e	0.0036	0.0095	-0.0014	0.0020	0.0005	1.3756
	O_3-C_f	0.0078	0.0243	-0.0040	0.0054	0.0014	1.3559
A-3	O_3-C_g	0.0077	0.0242	-0.0038	0.0050	0.0012	1.3219
A-4	C_3-C_h	0.0010	0.0038	-0.0004	0.0007	0.0003	1.6167
	C_2-C_i	0.0010	0.0037	-0.0004	0.0007	0.0003	1.6829
A-5	O_1-C_j	0.0077	0.0242	-0.0046	0.0054	0.0008	1.1681
	O_1-C_k	0.0078	0.0243	-0.0046	0.0053	0.0007	1.1436

Table S4. Resistance measurements and conductivity calculation of $SWCNT_{0.1}$ and $CG2_1$-$SWCNT_{0.1}$ in water and on solid (FP-coated) surface.

Sample Code	Conductance (μS, in water)[a]	Resistance (R) (kΩ)[b]	Conductivity (κ) (Sm^{-1})
$SWCNT_{0.1}$	0.42 ± 0.14	-	-
$CG2_1$-$SWCNT_{0.1}$	1.69 ± 0.55	7.36	0.4

[a]0.15 mL was diluted with 15 mL water and the conductance was measured. [b]Average resistance (R) recorded on the multimeter was 7356.6 Ω (for the coated area (W = 0.2 cm, L = 0.1 cm, T = 0.01462 cm); the calculated resistivity was ρ = 215.10 Ωcm (Eq. 1), corresponding to a conductivity of κ = 0.004 Scm^{-1} (Eq. 2).

Table S5. Resistance of $CG2_1$-$SWCNT_{0.1}$ coating on the FP after bending.

Entry	Number of bending cycles	Average resistance (kΩ)
1	0	7.36
2	2	27.67
3	4	48.0
4	10	537.0
5	20	999.66
6	30	1299.33
7	50	1550.66

5. Supplementary figures.

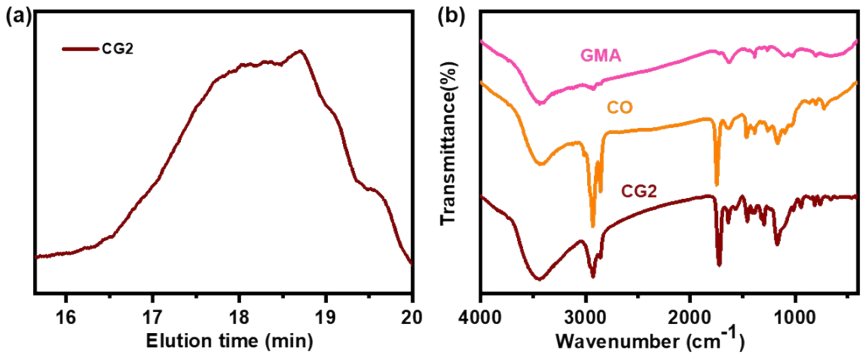

Fig. S1 (a) GPC chromatogram of CG2 and (b) FTIR spectra of CG2 preparation

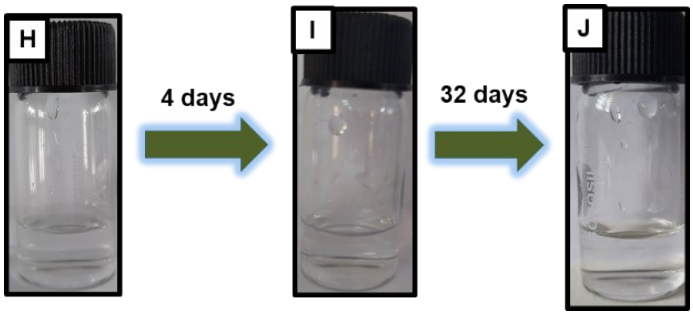

Fig. S2 Stability of the $CG2_{0.004}$-$SWCNT_{0.00002}$ solution on the 1st day (H), after 4 days (I), and after 32 days (J).

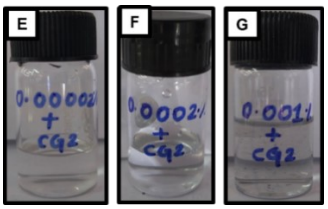

Fig. S3 Images of the vials containing aqueous solutions of (**E**) $CG2_{0.004}$-$SWCNT_{0.00002}$ (**F**) $CG2_{0.004}$-$SWCNT_{0.0002}$ (**G**) $CG2_{0.004}$-$SWCNT_{0.001}$.

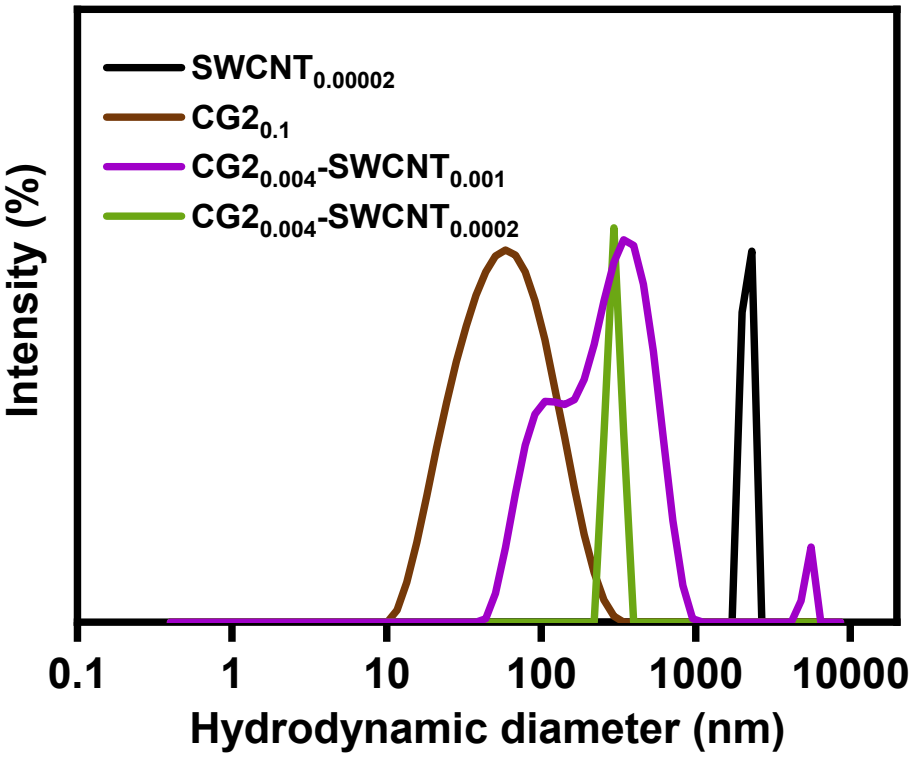

Fig. S4 DLS plots of SWCNT, CG2, and CG2–SWCNT dispersions.

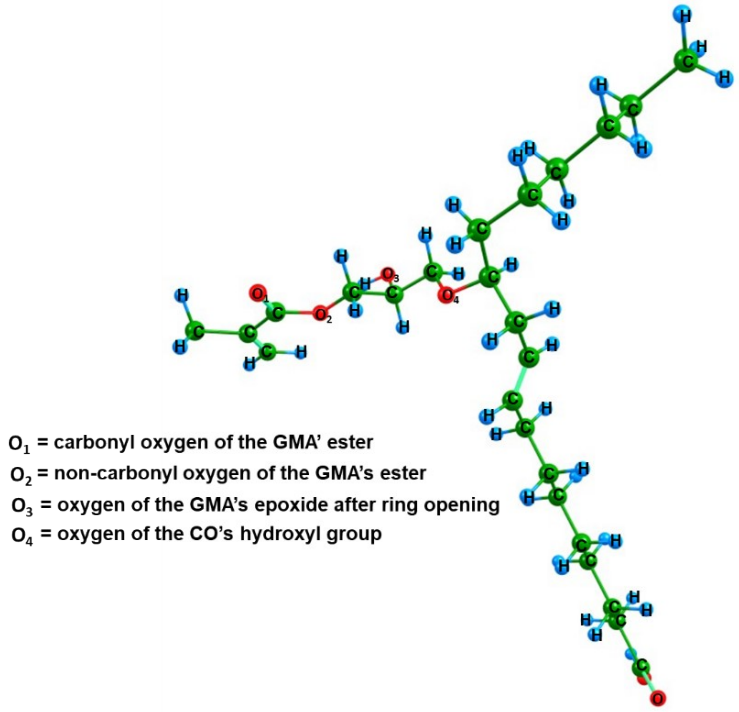

Fig. S5 Assignment of the four oxygens in the CG2*.

6. Supplementary Videos.

S1) Demonstration that uncoated FP is ineffective for touch-screen applications.

https://drive.google.com/file/d/1InzLBiEfRtnwqaRQ_55w-0fy65mduX5t/view?usp=drive_link

S2) Demonstration that $CG2_1$-$SWCNT_{0.1}$–coated FP, when attached to the fingertips of gloves, enables touch-screen operation.

https://drive.google.com/file/d/1Fj5-Zu0O7uR2YJZxA1jMlHr9-bBNPC6D/view?usp=drive_link

S3. Touchscreen application in cold conditions.

https://drive.google.com/file/d/1VmJDEstKSI5LgLZedAgsomzvZfxC57jr/view?usp=drive_link

References.

1. M. J. Frisch, G. W. Trucks, H. B. Schlegel, G. E. Scuseria, M. A. Robb, J. R. Cheeseman, G. Scalmani, V. Barone, G. A. Petersson, H. Nakatsuji, X. Li, M. Caricato, A. V. Marenich, J. Bloino, B. G. Janesko, R. Gomperts, B. Mennucci, H. P. Hratchian, J. V. Ortiz, A. F. Izmaylov, J. L. Sonnenberg, Williams, F. Ding, F. Lipparini, F. Egidi, J. Goings, B. Peng, A. Petrone, T. Henderson, D. Ranasinghe, V. G. Zakrzewski, J. Gao, N. Rega, G. Zheng, W. Liang, M. Hada, M. Ehara, K. Toyota, R. Fukuda, J. Hasegawa, M. Ishida, T. Nakajima, Y. Honda, O. Kitao, H. Nakai, T. Vreven, K. Throssell, J. A. Montgomery Jr., J. E. Peralta, F. Ogliaro, M. J. Bearpark, J. J. Heyd, E. N. Brothers, K. N. Kudin, V. N. Staroverov, T. A. Keith, R. Kobayashi, J. Normand, K. Raghavachari, A. P. Rendell, J. C. Burant, S. S. Iyengar, J. Tomasi, M. Cossi, J. M. Millam, M. Klene, C. Adamo, R. Cammi, J. W. Ochterski, R. L. Martin, K. Morokuma, O. Farkas, J. B. Foresman and D. J. Fox, *Journal*, 2016.
2. J.-D. Chai and M. Head-Gordon, *Physical Chemistry Chemical Physics*, 2008, **10**, 6615-6620.
3. R. F. W. Bader, *The Journal of Physical Chemistry A*, 2007, **111**, 7966-7972.
4. in *Discovering Chemistry with Natural Bond Orbitals*, 2012, DOI: https://doi.org/10.1002/9781118229101.ch9, pp. 209-230.
5. A. Ghosh, T. Debnath, T. Ash and A. K. Das, *RSC Advances*, 2017, **7**, 9521-9533.
6. E. R. Johnson, S. Keinan, P. Mori-Sánchez, J. Contreras-García, A. J. Cohen and W. Yang, *Journal of the American Chemical Society*, 2010, **132**, 6498-6506.
7. T. Lu and F. Chen, *Journal of Computational Chemistry*, 2012, **33**, 580-592.
8. W. Humphrey, A. Dalke and K. Schulten, *J Mol Graph*, 1996, **14**, 33-38, 27-38.
9. R. Padmanaban, D. Sen, S. M, E. S and J. Sarkar, *ACS Applied Bio Materials*, 2025, **8**, 6808-6816.